Ion Conducting Nanocomposite Membranes Based on PVA-HA-HAP for Fuel Cell Application: II. Effect of Modifier Agent of PVA on Membrane Properties

Elbadawy A. Kamoun[1,*], M. Elsayed Youssef[2], M. A. Abu-Saied[1], Alaa Fahmy[3], Hazem F. Khalil[3], Farag Abdelhai[3]

[1] Polymeric Materials Research Dep., Advanced Technology and New Materials Research Institute (ATNMRI), and
[2] Computer Based Engineering Applications Dep., Informatics Research Institute IRI, City of Scientific Research & Technological Applications (SRTA-City), New Borg Al-Arab City, 21934 Alexandria, Egypt
[3] Chemistry Dep., Faculty of Science, Al-Azhar University, 11884 Cairo, Egypt
[*]E-mail: badawykamoun@yahoo.com; e-b.kamoun@tu-bs.de

This work explores the synthesis and properties alteration of new nanocomposite membrane system based on polyvinyl alcohol (PVA) blended with hyaluronic acid (HA) and hydroxyapatite (HAP) as nanofiller. The membranes were synthesized by solution-casting method, where PVA was initially modified with orthophosphoric acid (OPA) or sulphuric acid and then epichlorohydrin (EPI) was employed as chemical crosslinker. Physicochemical properties of composite membranes *e.g.* gel fraction (%), swelling degree and mechanical stability were estimated, depending on PVA modifier agent alteration. Results revealed that the PVA-modifier agent type influenced sharply on most membrane properties. For example, the swelling ability of PVA-HA-HAP composite membranes was reduced apparently with increasing H_2SO_4 amount as used for PVA modification, unlike it was increased with the used amount of OPA for the same purpose. The mechanical properties were improved with increasing the amount of EPI until certain extent, whereas they have deteriorated controversially with addition of high incorporated amounts of HAP or using high amounts of OPA or H_2SO_4 for PVA modification. Meanwhile, electrochemical properties of PVA-HA-HAP composite membranes showed a big improvement in ionic conductivity with PVA modification and HAP incorporation as well. An one–dimensional matlab model is devoloped to study the performance of DMFC for different new composite membranes. Both experimatl and modeled performance of differnet membranes in DMFC were compared and discussed in details.

1. INTRODUCTION

Composite membranes as flexible materials have found diverse applications in biomedical and industrial fields simultaneously. The recent studies have shown an intrinsic improvement for membrane properties due to modified-clay inclusion into polymeric matrix. Inclusion of nano-particles as fillers with high portion ratio in organic polymers has been attracted much attentions and it has been extensively studied for long time. The combination between the organic part (*i.e.* polymer) and inorganic parts (*i.e.* filler) is as a result of collecting the advantages of two component system parts together [1]. For example, elasticity, flexibility, processability and chemical stability of polymer part, in addition thermal and mechanical stabilities, fire retardency, barrier properties and conductivity of filler part [2-5]. Polyelectrolyte membranes (PEM) or organic-nanofiller composite membranes can be fabricated by diverse synthetic routes; first, the organic component (*i.e.* polymer) has been incorporated as: precursor (*e.g.* monomer or oligomers), dissolved or suspended linear polymer, or crosslinked polymers network. Second, the inorganic part can be included for PEM as; precursor, or nano-sized particles. The chemical crosslinking was preferred to crosslink PEM, due to its operating in harsh conditions (*e.g.* high operating temperature upper 60 ^{o}C) which restrict the use of physical crosslinked PEM [4, 5]. Several of layered nano-particles are suited intensively to increase the permittivity properties, among them, semectite clays like montmorillonite (MMT) which is potentially used for designing a polymer nanocomposite [6]. Additionally, nano-sized MMT clays were previously used with PVA as filler not only to improve physicochemical properties of PVA-MMT membranes, but also to enhance the conductivity of PVA-MMT composite membranes for direct methanol fuel cells (DMFCs) [1]. Recently, hydroxyapatite (HAP) nano-particles are used for the same aforementioned purpose instead of MMT nano-clay, with PVA composite membranes for alkaline DMFC applications [7]. Several layered-fillers are perfectly suited for enhancing the barrier characteristics, among them smectite clays are frequently designed as composite membranes [6, 8]. An inorganic bioactive constituent such as, HAP nano-particles have been purposely merged with hydrogels to offer essential biological and mechanical properties [9]. Hydroxyapatite, HAP or calcium phosphate ($Ca_{10}(PO_4)_6 (OH)_2$, has been frequently employed formerly as scaffold or implanting materials in biomedical applications, due to its unique biological activity and physicochemical properties [10]. Furthermore, nano-HAP has superior specific surface area and excellent mechanical and biological properties [9]. Here, the purpose behind incorporation of HAP into PVA matrix allows reducing the glass transition temperature (T_g), the crystallinity degree, and thus increases the amorphous phase of the PVA polymer matrix, which then increases the ionic conductivity and the mechanical strength of obtained PEM.

Poly(vinyl alcohol) PVA, is a water-soluble polymer, it has been chosen as an organic part for PEM [5, 11]. PVA membranes are flexible materials and own high transparency, high dimensional stability and super permeability properties. PVA has been a known semi-crystalline polymer which possesses certain physical properties due to its crystal-amorphous interfacial effect [12]. PVA was previously used as polymer membranes for fuel cells. For example, Maiti et al.,[11] used crosslinked nanocomposite membranes of Nafion and PVA polyelectrolyte membranes for fuel cell applications. Nevertheless, PVA itself owns a destitute proton conductivity as compared to standard Nafion

membranes, because the PVA does not have any polyatomic anions for example, negative charged ions, such as –COO$^-$ or SO$_4^{2-}$ groups [5, 11, 13]. Thus, several reports showed the chemically modification of PVA polymer membranes with the orthophosphoric acid (H$_3$PO$_4$) [11, 14, 15], hypophosphorus acid (H$_3$PO$_2$) [16], heteropolyacids [17, 18], ammonium salts [19], dipotassium phosphate (K$_2$HPO$_4$) [20], or sulfuric acids and sulphosuccinic acid [11, 21] to limit the methanol crossover and to create the ionic conductivity at PVA for being a suitable PEM for fuel cell applications. Accordingly, the surface modification of PVA is an imperative step before its use for PEM for creating ionic surface conductivity [5, 11, 13].

Hyaluronic acid (HA) is a natural linear repetitions of di-polysaccharides, consisting of *β-(1, 4)-linked D*-glucuronic acid and *β-(1,3) N-acetyl-D*-glucosamine units. HA is a poly anionic polymer that owing diacritical properties and distinctive biological functions [22-24]. Here, the use of HA with PVA simultaneously as blended polymers in the organic part of PEM, is regarded a relative new idea after our first reported attempt [15]. Likewise, sodium alginate (SA) was blended with PVA based on ion conducting membranes for DMFC applications [17]. They demonstrated that addition of SA into PVA improved the efficiency of DMFC such as, selective water sorption and methanol barrier properties. Tafaoli-Masoule et al., [25] constructed the genatic algorithm to reach the optimum design parametrs and operating conditions needed for produce maximum power from DMFC's fuel. Yuan et al., [26] studied operational aspects of a passive DMFC incorporating an anodic methanol barrier. Bahrami et al., [27] reviewed a modeling and numerical simulation for DMFC. The results revealed that, many areas still need urgently efforts due to the dependency of various transport variables on capillary pressure. Ge et al., [28] developed a three-dimetional mathematical model for liquid feed-DMFC based on a Finite-volume technique. The results showed that the methanol crossover plays an important role even at a very low methanol concentrations and the cell performance reduced with increasing the obtained current density. While, the anode catalyst-layer porosities and the diffusion layer have a considerable impact on methanol crossover and the entire cell performance. Liu et al., [29] constructed a three dimentional, two phase model for (DMFC) using commercial software fluet. The numerical results revealed that the low methanol transport is owing to the land effect and nonuniform current density distribution affected by spatially distributed methanol crossover rate.

The present work focuses on developing ionic-conducting composite membranes based on PVA-HA-HAP system for fuel cell application. We demonstrated the available feasibility of PVA-HA-HAP composite membranes obtained through chemical crosslinking by EPI with investigating the swelling degree, effect of modifier agent type of PVA and HAP incorporation on the resultant membrane properties. In addition, the Matlab model was used to compare the experimental and mathematical data of PVA-HA-HAP membranes performance to be employed for DMFC applications.

2. EXPERIMENTAL

2.1. Materials and Methods

PVA (typically average M$_{wt}$ 72,000 g/mol; 98 % hydrolyzed) was obtained from Merck, Germany. Hyalouronic acid (HA) was purchased from Shanghai Jiaoyuan Industry Co., Ltd., China. Hydroxyapatite, (HAP) (nano powder, OD > 200 nm, purity 99.9 %) obtained from Nano Inglobal,

China. Orthophosphoric acid, (OP) (M_{wt} 98 g/mol; 85% purity; density 1.691~1.721 g/mL) was obtained from Poch, Poland. Epichlorohydrin, (EPI) (99.5%) was obtained from Fluka Chemie, Germany.

2.2. Gel fraction and water uptake

The resultant PVA-HA-HAP composite membranes are vacuum-dried at room temperature for 12 h to avoid any surface shrinking, weighted (W_0), and then immersed in distilled water for further 24 h up to an equilibrium swelling weight (W_s), for removing the leachable or any soluble HA parts from membrane. The composite membranes are then vacuum-dried and weighted again (W_e). The gel fraction (GF %) was carried out according to the method reported by Yang et al., [30] and calculated by the following equation (1).

Gel fraction (GF %) = (W_e / W_0) ×100. (1)

Where, (W_0) and (W_e) are the weights of dried membrane samples before and after soaking, respectively.

The water uptake of the PVA-HA-HAP membranes is usually defined in weight percent with respect to the weight of the dried membrane. For measuring the swelling ability of PVA-AH-HAP composite membranes, membrane samples were cut into 3.5 cm × 3.5 cm pieces and vacuum-dried for 12 h, the dried sample weight is determined (W_{dry}). The dried membranes were immersed in distilled water at RT, then weighted (W_{wet}) at specific interval times. The water uptake of PVA-HA--HAP membranes was given as equation (2) [31].

Water uptake (%) = [(W_{wet} − W_{dry}) / W_{dry}] × 100. (2)

2.3. Ionic Conductivity

Proton conductivity measurements of PVA-HA-HAP composite membranes were performed and sandwiched between two stainless steel electrodes-AC impedance method, (impedance gain-phase analyzer; model 1260A, Solatron Analytical, UK). The membrane is cut into this dimension (2.0 cm wide × 6.0 cm long), the membrane is immersed in de-ionized water for 12 h before the test, then vacuum-dried and the thickness is digitally determined. The measurements are conducted in 100% humidity (fully hydrated) by leaving the deionized water at the bottom of the glass container reactor, at 25-50 ^{o}C, AC impedance spectra of tested samples are monitored in frequency about 1-10 MHz and 10 mV amplitude. The ionic conductivity of membranes can be calculated using the given equation 3.

$\sigma = l\ (RA)^{-1}$ S cm^{-1}. (3)

Where, σ is the ionic conductivity of membrane, l is the thickness of membrane in cm, R is the resistance of the membrane, and A is the membrane cross-section area in cm^2 [9].

2.4. Testing of membranes in PEM-fuel cell test station

The membrane efficiency toward its use for fuel cell application was assessed in PEM-fuel cell test station (GREENLIGHT, CA) using membrane electrode assembles method. Teflon-carbon papers

(0.75 mm thickness) were used as backing layers for the two electrodes. Pt-Ru (50 wt. %, 1:1) was supported on one of the gas diffusion layer anode electrode, while Pt (50 wt. %) was supported on the other electrode (cathode) to maintain the loaded catalyst on both electrodes 1 gm cm^{-2}. The cell test station was operated at 55 ^{o}C, using 2 *M* methanol's aqueous at anode part, and oxygen at cathode part under room pressure.

2.5. Preparation of PVA-HA-HAP Nanocomposite Membranes
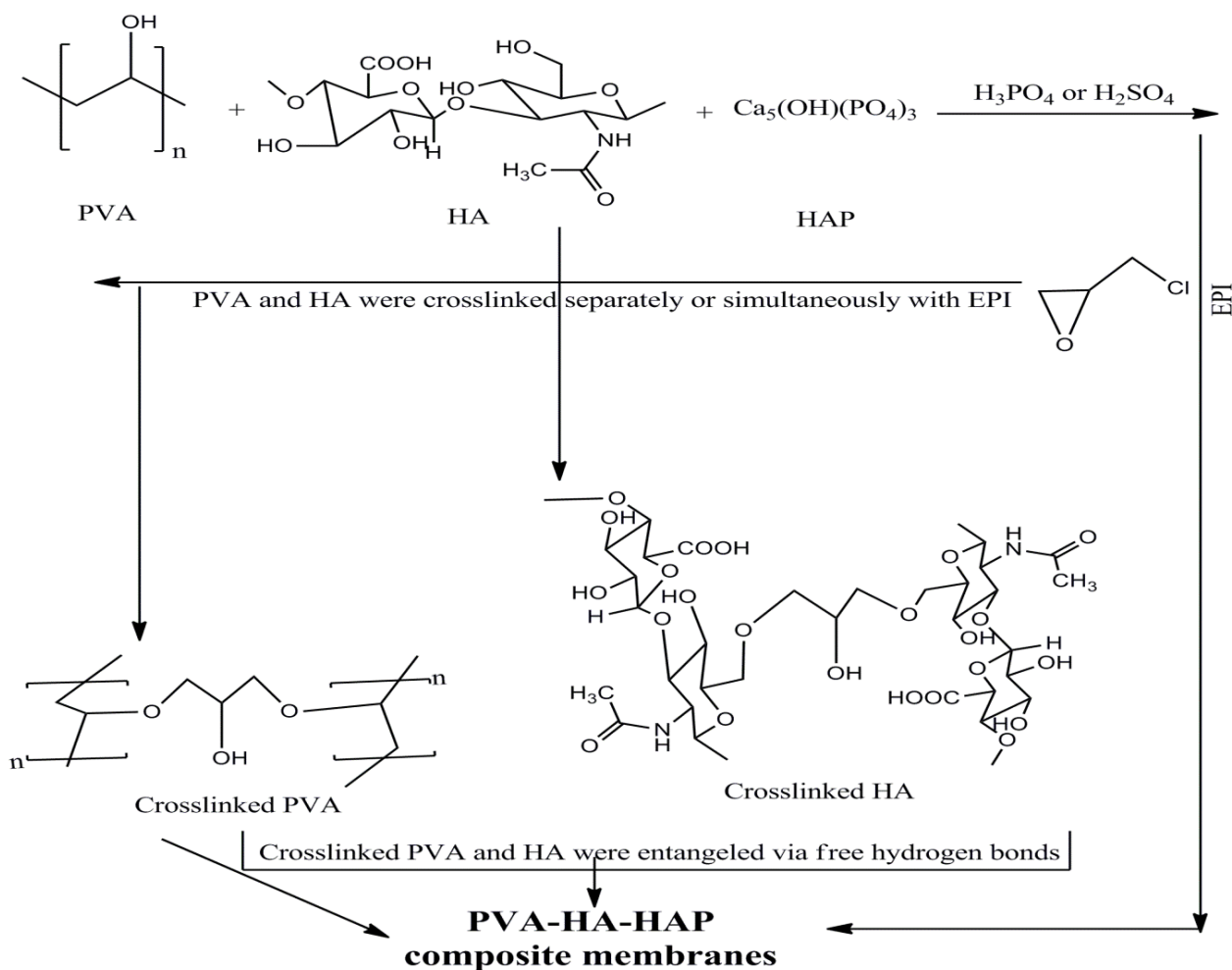

Scheme 1. Schematic depiction showing the synthesis route of PVA-HA-HAP composite membranes.

PVA-HA-HAP composite membranes were prepared by solution-casting method. Typically, 30 g of PVA powder is dissolved in 270 ml distilled water with continuous stirring at 60 ^{o}C for 2h getting 10 wt. % polymer solutions. The solution is kept at room temperature according to the reported procedure of Liang et al. [32]. One gram of hyaluronic acid powder is dissolved in 49 ml of distilled water with continuous stirring at room temperature for one hour getting 2 wt. % HA solution. Aqueous solution containing 10 wt. % of PVA is allowed to react with orthophosphoric acid for PVA modification. OPA modifier agent is added to PVA solution step-wise (during a half hour) with continuous stirring at 40 ^{o}C for one hour,[16] followed by different concentrations of HA (0.5, 1, 1.5,

and 2 wt. %) are added with aforementioned conditions for one hour, where the ratio of PVA: HA is 4 : 1. Different amounts of HAP (0.5, 1, 2, 3, 4, 6, and 8 wt. %), is dispersed into the bulk solution under harsh stirring for 4h. The polymer- nano-filler bulk solution is sonicated for one hour to ensure the homogeneity among compositions and to remove formed air bubbles. EPI with different ratios (0.1, 0.25, 0.5, 1, 2, 4, and 5, v/v, %) are added for crosslinking the two polymers. The bulk solution is kept under stirring for one hour till the mixture becomes a homogenous viscous appearance at 60 ^{o}C, followed by sonicated again. The PVA-HA-HAP solution was poured gently to plastic Petri-dish with diameter 14 cm. The membrane thickness is adjusted by using 20 ml of the poured bulk solution. The plastic dish is remained at room temperature for 24 h, and then carefully incubated in humidity-chamber to adjust the evaporation step of solvent. Finally, membranes are then vacuum-dried at room temperature for 4 h, (scheme 1). The dried PVA-HA-HAP membranes are kept in vacuumed-plastic bags to avoid the moisture exposure for storage till use.

2.6. Mathematical model

Two catalyst layers and membrane are considered in the following model. Voltage loss is considered for both catalyst layers and membrane. One dimensional model for polarization curves of cell is introduced in which neglect reactant transport in the feed channel. Scheme 2 shows sketch diagram of DMFC components with methanol and oxygen concentration gradients.
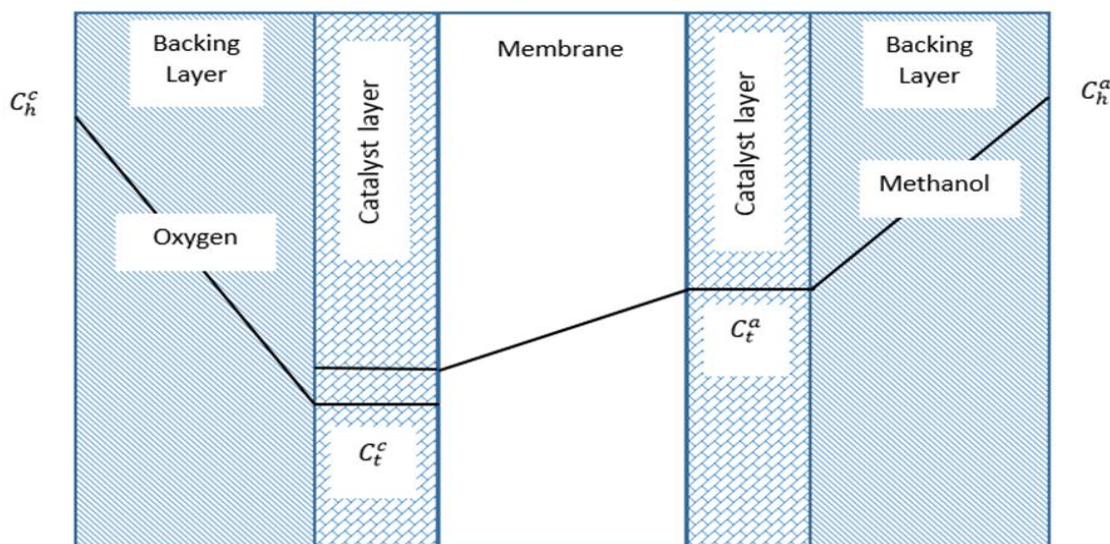
Scheme 2. Sketch diagram of DMFC components with methanol and oxygen concentration gradients.

$$V_{cell} = \eta_{oc} - \eta_o^a - \eta_o^c - \frac{j_o L_m}{\sigma_m} \qquad (4)$$

Where V_{cell} is cell voltage, η_{oc} is theoretical ideal cell voltage, η_o^a over potential at anode, η_o^c over potential at cathode, j_o is proton current density, L_m is the membrane thickness and σ_m is the membrane conductivity.

Over potential at anode according to small and high current density

$$\frac{\eta_o^a}{\eta_*^a} = \ln\left(\frac{j_o}{j_*^a}\right) - \ln(k^a) - \gamma^a \ln\left(1 - \frac{j_o}{j_{lim}^a}\right) + \gamma^a \ln\left(1 + \beta + n_d \frac{j_o}{j_w}\right), j_o \ll j_*^a \qquad (5)$$

$$\frac{\eta_o^a}{\eta_*^a} = 2\ln\left(\frac{j_o}{j_*^a}\right) - \ln(k^a) - \gamma^a \ln\left(1 - \frac{j_o}{j_{lim}^a}\right) + \gamma^a \ln\left(1 + \beta + n_d \frac{j_o}{j_w}\right), j_o \gg j_*^a \qquad (6)$$

Where j_*^a is a characteristic protons current, γ^a is order of reaction at anode, and n_d is drag coefficient.

$$\eta_*^a = \frac{R\,T}{\alpha^a\,F}, \quad j_*^a = \frac{2\,\sigma^a\,\eta_*^a}{L_t^a}, \quad k^a = \frac{L_t^a\,L_*^a}{j_*^a}\left(\frac{C_h^a}{C_{ref}^a}\right)^{\gamma^a} \qquad (7)$$

$$\beta = \frac{D_m L_b^a}{D_b^a\,L_m}, \quad j_{lim}^a = \frac{6\,F\,D_b^a\,C_h^a}{L_b^a}, \quad j_w = \frac{F\,D_b^a w^a}{L_b} \qquad (8)$$

Where, R is gas constant, T working temperature, α^a is transfer coefficient at anode, F is Faraday constant, σ^a is proton conductivity at anode, L_t^a is catalyst layer thickness at anode, C_h^a is molar concentration at anode, D is diffusion coefficient, and w^a is molar concentration of water at anode side. Superscripts (a) mean at anode side and (c) mean at cathode side and subscript (*) mean characteristic value and (m) is mean membrane.

Over potential at cathode according to small and high current density is identified as follows:-

$$\frac{\eta_o^c}{\eta_*^c} = \ln\left(\frac{j_o}{j_*^c}\right) - \ln(k^c) - \gamma^c \ln\left(1 - \frac{j_o}{j_{lim}^c} - r_{cross}\right), j_o \ll j_*^c \qquad (9)$$

$$\frac{\eta_o^c}{\eta_*^c} = 2\ln\left(\frac{j_o}{j_*^c}\right) - \ln(k^c) - \gamma^c \ln\left(1 - \frac{j_o}{j_{lim}^c} - r_{cross}\right), j_o \gg j_*^c \qquad (10)$$

Where,

$$\eta_*^c = \frac{R\,T}{\alpha^c\,F}, \quad j_*^c = \frac{2\,\sigma^c\,\eta_*^c}{L_t^c}, \quad k^c = \frac{L_t^c\,L_*^c}{j_*^c}\left(\frac{C_h^c}{C_{ref}^c}\right)^{\gamma^c}, \quad j_{lim}^c = \frac{4\,F\,D_b^c\,C_h^c}{L_b^c} \qquad (11)$$

$$r_{cross} = \frac{j_{lim}^a}{j_{lim}^c}\left(\frac{\beta + n_d \frac{j_o}{j_w}}{1 + \beta + n_d \frac{j_o}{j_w}}\right)\left(1 - \frac{j_o}{j_{lim}^a}\right) \qquad (12)$$

2.7. Characterization and Instrumentation

FTIR spectra were recorded by (EQUINOX 55, BRUKER Germany) using KBr transparent discs. IR spectra were recorded at 64 scans between 4000–400 cm^{-1} with a resolution of 2 cm^{-1}. Vacuumed-dried samples were pressed by applying a force 105 N into transparent disk (disk weight and diameter ~ 125 mg and 14 mm), respectively. KBr-sample discs were measured in the absorbance mode. The mechanical stability measurements of composite membranes *e.g.* the maximum tensile-strength and the elongation-at-break were carried out with a universal tensile testing machine (model: AG-I/ 50N-10KN, Japan). PVA-HA-HAP membranes were cut into the specific shape of a dog-bone-shape-dimension (~ 5 cm long × 1.5 cm wide-the ends × 1 cm middle). The measurements were carried out at stretching rate 10 mm/min with pre-load of 0.5 N to determine load for each sample. Thermogravimetric analysis (TGA) and differential scanning calorimeter (DSC) thermograms were carried out with a 204 Phoenix TGA/DSC instrument (NETZSCH, Germany), at a heat-scan rate 5 °C min^{-1} at 25–600 ^{o}C in N$_2$ for TGA and 10 °C min^{-1} at 25– 400 °C with N$_2$ gas for DSC analysis.

3. RESULTS AND DISCUSSION

3.1. FT-IR

Fig.1 shows IR spectra of the neat PVA, PVA-HA, and crosslinked PVA-HA-HAP membranes crosslinked by EPI. The recorded IR spectra present the dominant –CH stretching vibrations of the polymer backbone as –CH (as/sym) stretches were observed in the spectral range 2916–2844 cm^{-1}[33]. As reported, the absorption bands of pristine PVA appeared at 3734 cm^{-1} for –OH free groups (unreacted and non-bonded groups), while intramolecular and intermolecular hydrogen bonds among –OH groups in PVA chains due to high hydrophilicity stretching bands were observed at υ 3389 cm^{-1} respectively [31]. It clearly reveals the intermolecular hydrogen bonding interactions between the produced polymers with terminal hydroxyl moieties owing to a red shift and the broadening of –OH stretch ranged 2500–3600 cm^{-1} in case of PVA and PVA-HA and in the presence of HAP. Therefore, the CH stretch expected at 2900-3150 cm^{-1}) was barely observed around 2924 cm^{-1}, however the broad shoulder nearby 2600 cm^{-1} is ascribed to a combination band (C=O stretch and –OH out-of-plane deformation). A broad C–H stretching band appeared at 2924 cm^{-1}, and bending –CH$_2$ bands appeared at 1429 cm^{-1}. Stretching bands for C=O groups remained from unconverted polyvinyl acetate into PVA appeared at υ 1678 cm^{-1} and 1560 cm^{-1}. Moreover, high intensity absorption band appeared at υ 1097 cm^{-1} indicates the crystallization or entanglement degree of PVA [31].

For more details, in case of PVA-HA, the wide band observed at 3410 cm^{-1} which can be attributed to the –OH stretch mode of HA and the band at 2912 cm^{-1} was the asymmetric stretching of C–H groups [34]. In addition bands at 3271 cm^{-1} is due to both –NH$_2$ group in glucosamine unite and bands at 1676 cm^{-1} corresponding to C=O (–COOH group) in guluronic acid residues unit of HA. Moreover, the absorption band at 1568 cm^{-1} indicates the presence of C=O related to (–COOH groups) of orthophosphoric acid at modified PVA. The intensity values of O–H out of plan motion were

reduced significantly, owing to further hydrogen bonding reaction occurred between PVA and HA. From aforementioned results, these spectral changes of –OH stretch mode are evidence also the covalent bind between –OH of HA and epichlrohydrine. Furthermore, bands at 1329, 1419 cm^{-1} might be related to C–C groups of PVA or HA.
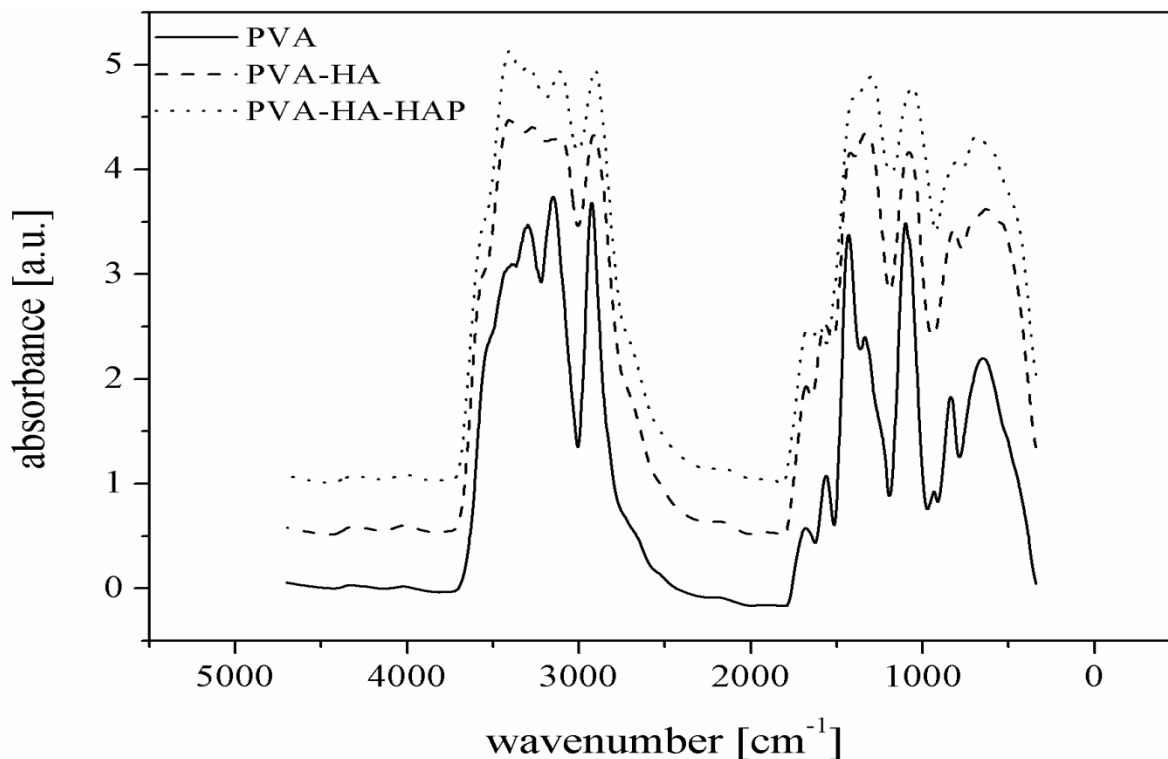
Figure 1. FTIR spectra of PVA (a), PVA-HA membranes (b), and PVA-HA-HAP nanocomposite membranes (c).

3.2. Effect of OPA of PVA modification on PVA-HA-HAP membrane properties

The study of swelling ability or water sorption degree of membranes was previously reported in most related literatures [17, 35]. The swelling degree and gel fraction (%) for PVA-HA-HAP composite membranes, their PVA was modified with different concentrations of OPA were presented in Table 1. The swelling measurement was conducted at room temperature in distilled water. It is noteworthy that, the PVA modification with OPA has influenced sharply on the swelling degree of composite membranes, nevertheless it has a relatively slight influence on the GF %. The resultant swelling data refers that, OPA might act as a secondary crosslinker beside the usual used ones (*i.e.* EPI), where OPA might be utilized as catalyst for crosslinking reaction [36, 37]. Thus, the swelling degree decreased progressively with increasing the crosslinking density of composite membranes, while the GF% was clearly increased slowly.

Table 1 shows also the mechanical properties data (*e.g.* maximum tensile strength and elongation-at-break %) for the PVA-HA-HAP membranes, their PVA was modified with different

OPA concentrations. It is clear that the tensile strength values were found unstable trend, while the elongation percentage of composite membranes increased dramatically with the modification of PVA without deterioration, owing to increasing the stiffness structure which was caused by the high crosslinking density of membranes.

Table 1. Effect of OPA concentrations as PVA modifier agent on physicochemical properties of PVA-HA-HAP composite membranes

OPA concentrations (v/v, %)	Gel fraction and swelling		Mechanical properties	
	GF (%)	Water uptake (%)	Tensile strength (Mpa)	Elongation-at-break (%)
0.5	48	623	30	145
1.0	46	525	25	166
1.5	45	280	15	330
2.0	47	225	14	349
2.5	46	158	14	344
3.0	45	140	19	380
3.5	42	52	16	430

Table 2. Effect of sulfuric acid concentrations as PVA modifier agent on physicochemical properties of PVA-HA-HAP composite membranes

H_2SO_4 concentrations (v/v, %)	Gel fraction and swelling		Mechanical properties	
	GF (%)	Water uptake (%)	Tensile strength (Mpa)	Elongation-at-break (%)
0.1	48	504	27	90
0.25	47	475	23	121
1.5	50	108	12	348
2.0	51	86	9	353
2.5	49	102	7	312

3.3. Effect H_2SO_4 of PVA modification on PVA-HA-HAP membrane properties

Table 2 shows the total water uptaken in PVA-HA-HAP composite membranes depending upon the PVA modification with different used amounts of H_2SO_4. As shown, the maximum water uptake values decreased with increasing the PVA modification with H_2SO_4, indicating that more crosslinking densities were formed which might lead to more rigid and more compact membranes interior structure. The dual role of H_2SO_4 as a secondary crosslinker beside its basic role as a modifier agent was observed as OPA. The task of H_2SO_4 as modifier agent for PVA was first detected by Maiti et al. [11], who found the swelling degree of membranes were sharply reduced by increasing the crosslinking degree or H_2SO_4 contents which maintain the tight contact between electrolyte membranes and catalyst. Boroglu et al. [38] have used fuming sulfuric acid as the sulfonating reagent for getting proton-exchange PVA membranes for DMFC. The GF % values show almost stable behavior, regardless of H_2SO_4 used concentrations. Table 2 indicates the mechanical properties of

PVA-HA-HAP membranes. It can be easily noticed that, the tensile strength of composite membranes decreases sharply in a stable-rate, as the concentration of H_2SO_4 increases. However, the elongation-at-break (%) of composite membranes increases also in a stable-rate up to (2 v/v, %. of H_2SO_4), then returns to decreases again. This behavior can be attributed to the fact that, the high concentration of used H_2SO_4 acid in PVA modification might lead to deterioration of the main polymer structure chains, which has further evidenced by the swelling degree increased unexpectedly after (2 v/v, % of H_2SO_4). This opposite behavior of acid modifier agent has not been detected in the case of PVA modification with OPA.
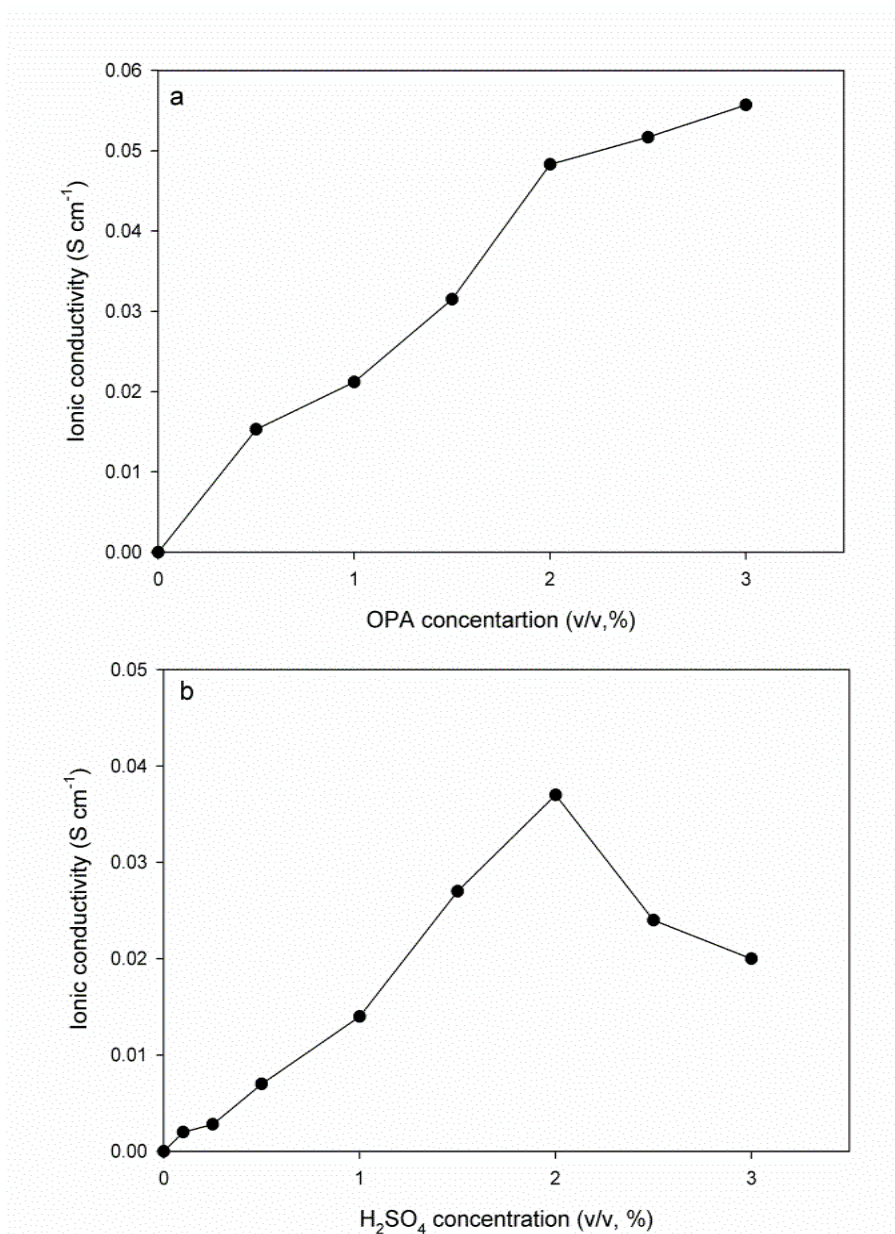
3.4. Ionic conductivity

It was suggested that, the PVA modification with OPA or H_2SO_4, is regarded the primary factor to generate and improve the proton conductivities [11, 13, 16]. This might be due to the fact that, the OPA or H_2SO_4 is the donor and the carrier of negative charged groups (PO_4^{3-} or $-SO_3^-H^+$, respectively) which are basically responsible for proton conductivity presence. The ionic or protonic conductivity measurements of PVA-HA-HAP composite membranes as function of different concentrations of OPA or H_2SO_4 (0, 0.5, 1.0, 1.5, 2, 2.5 and 3.0 v/v, %), were presented in Fig. 2a and b, respectively. As seen, the proton conductivity values range progressively from 0–0.057 S cm^{-1}, owing to the modification of PVA with OPA from 0–3.0 (v/v, %), (Fig. 2a). Likewise, the proton conductivity values increase dramatically in the range from 0–0.038 S cm^{-1}, when the PVA was modified by varied H_2SO_4 concentrations from 0–2.0 (v/v, %), then the ionic conductivity return to decrease again with H_2SO_4 concentration > 2.0 (v/v, %), (Fig. 2b). The obtained results of proton conductivity are typically consistent with reported results of Rhim et al. [5], they explored that the protonic conductivities of modified PVA membranes with sulfosuccinic acid improved significantly, due to increase the number of charged negative ions ($-SO_3^-H^+$ groups) which were responsible to protonic conductivity generation. These directories concludes that, the proton conductivity values increase with increasing the introduced negative charges (*i.e.* PO_4^{3-} or $-SO_3^-H^+$) of modifier agent either OPA or H_2SO_4 within PVA polymer matrix, while the PVA modification with H_2SO_4 gave a relatively protonic conductivity reduction, particularly with H_2SO_4 concentration greater than 2 (v/v, %). The distinction of ionic conductivity results related to the type of modifier agent of PVA and dependence the electrochemical membranes properties on the acid modifier agent and type, as lately discussed by Gupta et al., [16] and Fernandez et al.[13]. They found that the ionic conductivity of fully hydrated membranes of PVA modified with H_3PO_4 or H_3PO_2 respectively, increases significantly with the acid content increases, nonetheless the negative effect on mechanical membrane properties.

### 3.5. Testing composite membranes on PEM-fuel cell station

3.5.1. Experimental and modeled numerical data

The PEM fuel cell performance curves of Nafion 117 as standard membrane, PVA-HA (non-modified and modified PVA with OPA) and PVA-HA-HAP composite membranes (their PVA were

modified with OPA), were collected and presented in Fig. 3, as experimental and modeled numerical data simultaneously. As shown, the peak power density of PVA-HA (non modified-PVA) is very negligible and near to zero value. However, the peak power density of PVA-HA (modified PVA) is 24 mW cm^{-2} at a load current density of 165 ~ mA cm^{-2}. Nonetheless, the peak of power density of PVA-HA-HAP composite membrane increased significantly to 90 mW cm^{-2} at a load current density of 300 mA cm^{-2}. The power density improvement of membranes can be ascribed to both the PVA modification with H_3PO_4 and the addition of HAP nano particles into PVA-HA polymer composition. It is noteworthy that, the proton conducting channels offered by the hydrated phase of HAP incorporation, in addition the proton conductivity has clearly improved with the modification of PVA by H_3PO_4 due to introduction of the negative charged conducting groups (Fig. 3).


Figure 2. The ionic conductivity of PVA-HA-HAP composite membranes, as function of different used amounts of modifier agents of PVA modification, OPA (a), and H_2SO_4 (b), all membranes were measured at 55 ^{o}C.
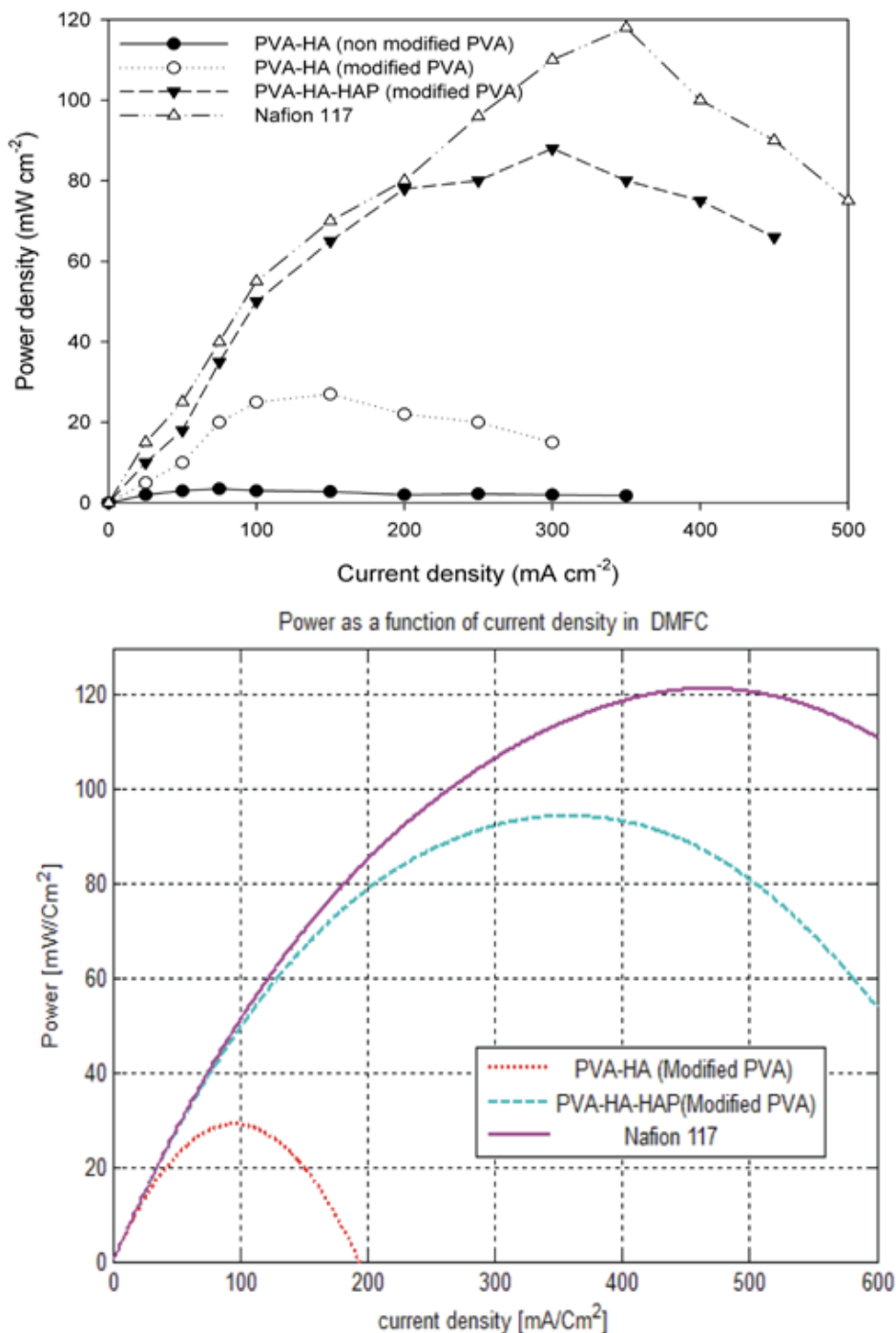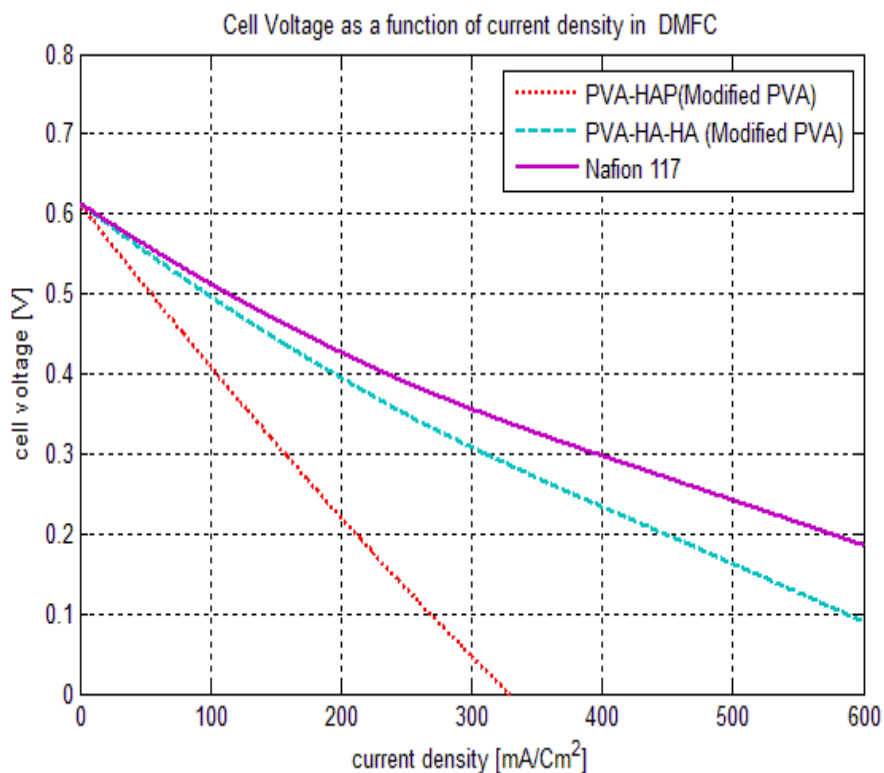
Figure 3. Power density against current density measured by PEM-fuel cell station for standard Nafion 117 membrane, PVA-HA membrane and PVA_{OPA}-HA-HAP composite membrane (experimental data, up) and (modeled numerical data, down).

These results are coincided with the presented results of proton conductivity in Fig 2. Similarly, our speculation of the improvement of both cell performance and ionic conductivity with PVA modification and HAP introduction, are fully consistent with published results of Mohanapriya et al.[17]. They demonstrated that a considerable improvement in cell performance was observed after PVA modification with hetero-polyacids of PVA-sodium alginate membranes as DMFC membrane.
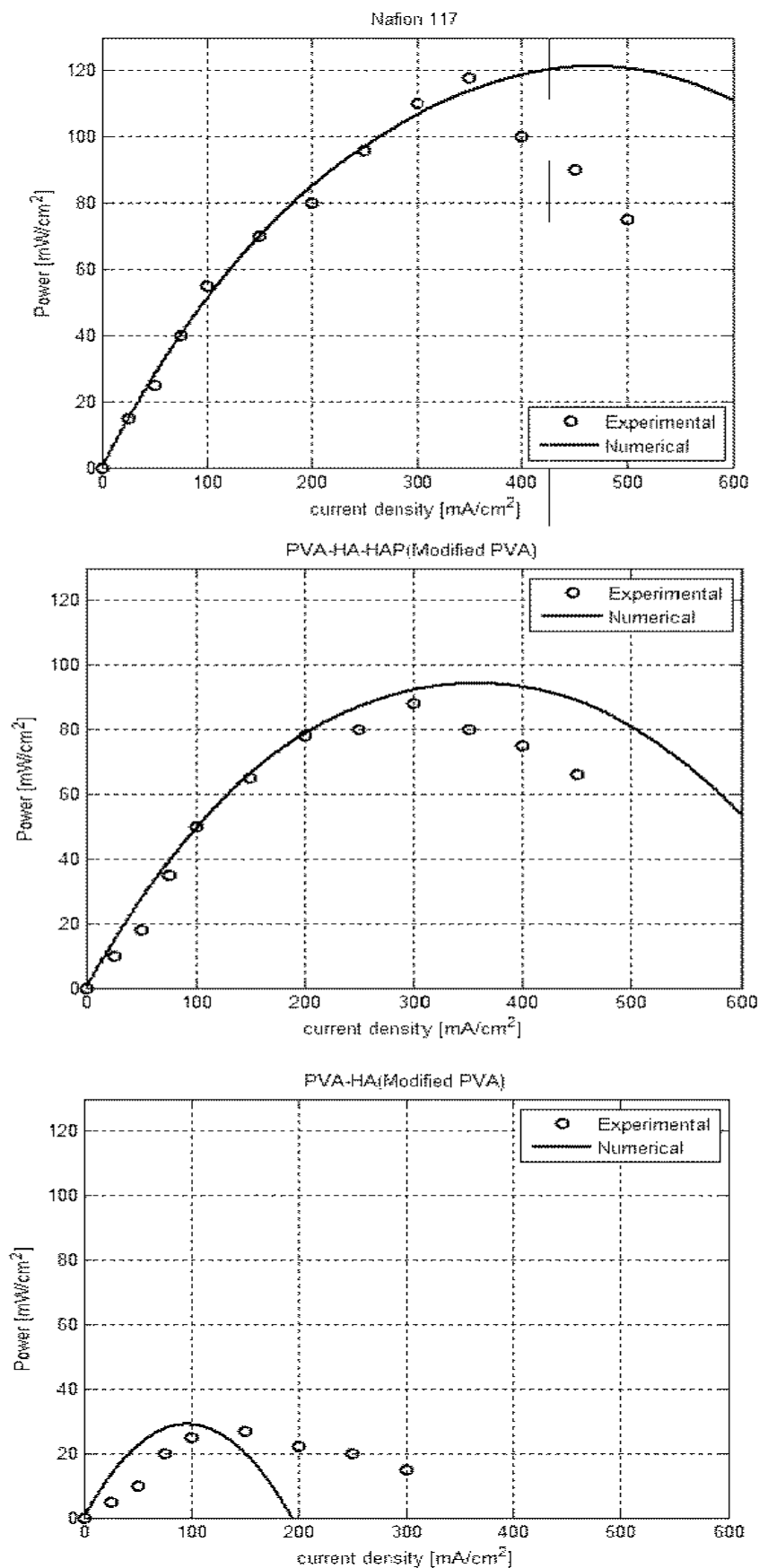
Figure 4. Comparison between experimental and modeled numerical data representing relation of power density against current density for Nafion 117 membrane (up), PVA$_{OPA}$-HA-HAP composite membrane (middle), and PVA$_{OPA}$-HA membrane (down).

Figure 5. Theoretical polarization curves for the three different DMFC membranes, (Nafion 117 membrane, PVA_{OPA}-HA-HAP composite membrane, and PVA_{OPA}-HA membrane).
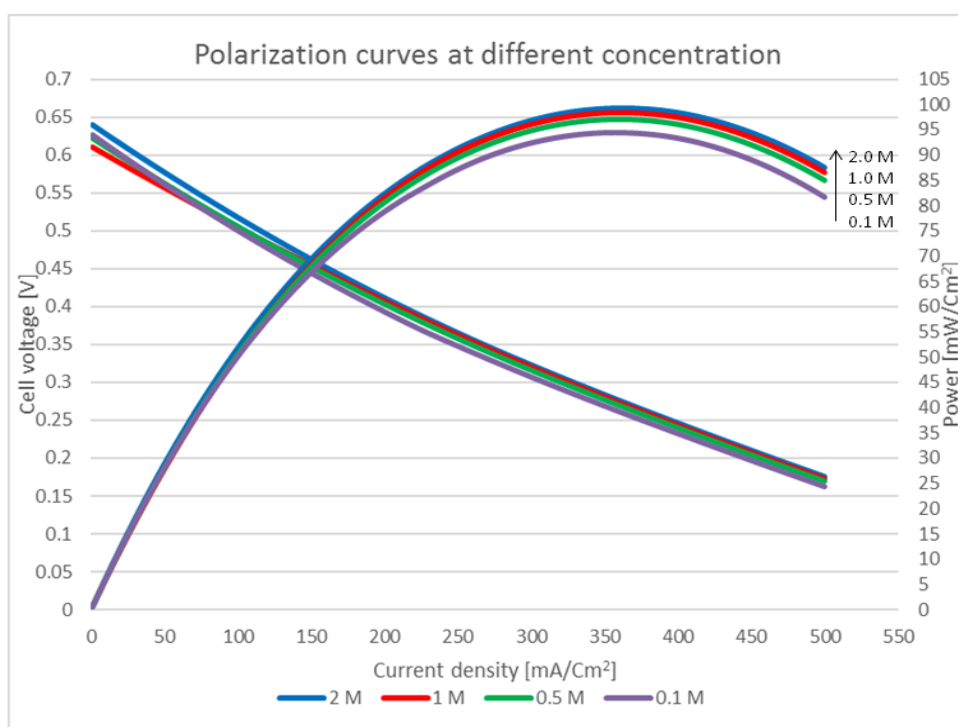
Figure 6. Theoretical power density and polarization curves vs. current density for PVA-HA-HAP composite cell membrane at different methanol feed concentration at cell barrier.

Figure 4 shows comparison between experimental and modeled numerical data of power density *vs.* current density for three composite membranes Nafion 117, PVA$_{OPA}$-HA-HAP (modified PVA with OPA), and PVA$_{OPA}$-HA, respectively. Cell temperature was operated at 55 ºC, methanol feed concentration is 2M, fuel pressure adjusted at 1 atm. and air pressure 2 atm., while the cathode pressure was 2 atm. and anode pressure was 1 atm. for both experimental measurements and numerical simulation calculations. In case of Nafion 117 membrane, the maximum power density obtained from the experimental measurements is 119 mW/cm^2 at current density ~ 345 mA/cm^2, while the calculated maximum power density is 121 mW/ cm^2 at current density is 450 mA/cm^2. In case of PVA$_{OPA}$-HA-HAP composite membrane, the maximum measured power density is 88 mW/ cm^2 at 300 mA/cm^2 cell current density, whereas the numerical simulation calculation is significantly offered that power density is 94 mW/ cm^2 at 360 mA/cm^2 cell current density. In case of PVA$_{OPA}$-HA membrane, the maximum power density is 27 mW/ cm^2 measured result at 150 mA/cm^2 cell current density, while the maximum predicted power density is 28 mW/ cm^2 at 100 mA/cm^2 cell current density. Interestingly, in case of Nafion 117 membrane and PVA$_{OPA}$-HA-HAP composite membranes, the deviation between experimental data compared by numerical results increase at higher current density that is owing to the numerical simulation model doesn't take into consideration the methanol crossover phenomena and the contact resistance between the two electrodes and the membrane is not considered, so that at higher current density the numerical results are higher than experimental measured results. The obvious conformity between the calculated data and experimental results has obtained at low current density for both Nafion 117 and PVA$_{OPA}$-HA-HAP composite membranes. In case of PVA$_{OPA}$-HA membrane, the quasi-agreement between the numerical results compared by experimental data at low current density was observed. Notably, the membrane of PVA-HA (non modified PVA) could not be numerically studied; because of the conductivity of non modified PVA is almost equal zero [5, 11, 13, 15].

Figure 5 shows the predicated results of DMFC cell voltage vs. current density for three composite membranes Nafion 117, PVA$_{OPA}$-HA-HAP, and PVA$_{OPA}$-HA at the same cell conditions as aforementioned. Both figures 4 and 5 of theoretical data of power density and cell voltage vs. current density indicate that the good performance of PVA-HA-HAP (modified PVA) as membrane for DMFC. Figure 6 illustrates power density and polarization curves *vs.* current density for PVA-HA-HAP (modified PVA) cell membrane at different methanol concentrations 0.5 M, 1 M, 1.5 M and 2 M, respectively. It is noticed that the increase of methanol concentration increases appreciably the cell voltage and cell power density. It is shown that, the maximum cell power density is 95 mW/ cm^2 at 0.5 M methanol concentration, while it reached to 100 mW/ cm^2 at 2 M methanol concentration.

4. CONCLUSIONS

In summary, our findings indicate that the composite membranes of PVA-HA-HAP were fabricated using a solution casting method, while chemical crosslinking was accomplished by EPI crosslinker. All fabricated composite polymer membranes influenced sharply by PVA modification process and HAP incorporation. As such, swelling ability and thermal stability of composite

membranes were reduced significantly with increasing the used amount of PVA modifier agent either OPA or sulfuric acid. On the contrary, electrochemical properties of composite membranes *e.g.* ionic conductivity and power density were enhanced progressively by PVA modification step with OPA and HAP incorporation. The improved conductivity and high performance of PVA-HA-HAP composite membranes at slightly elevated temperature (at 55 ^{o}C) are the main advantages for commercialization of fuel cell, motivating efforts to increase the efficiency of membranes by suitable modification for PVA or HAP nanofiller incorporation. One–dimensional matlab mathametical model has been used to investitgate the mass transport with electrochemical reacting occuring in the DMFC by using three new composite membranes. The calculated results elucidated that the high performance of using PVA$_{OPA}$-HA-HAP membrane (modified PVA with OPA), as DMFC membrane compared by its cost with standard membrans such as, Nafion 117 membranes. According a practical point of view, the PVA-HA-HAP composite membranes could be easily fabricated by a simple blending and crosslinking processes. The PVA-HA-HAP composite membranes are a proper candidate for DMFC application, due to their excellent electrochemical properties and low cost as compared to standard commercial Nafion membranes.

References

1. C.-C. Yang and Y.-J. Lee, *Thin Solid Films* 517 (2009) 4735
2. E. A. Kamoun, and H. Menzel, *J. Polym. Res.*, 19 (2012) 9851
3. B. P. Tripathi, and V.K. Shahi, *Prog. Polym. Sci.*, 36 (2011) 945
4. P. Duangkaew, and J. Wootthikanokkhan, *J. Appl. Polym. Sci.*, 109 (2008) 452
5. J.-W. Rhim, H. B. Park, C.-S. Lee, J.-H. Jun, D. S. Kim, and Y. M. Lee, *J. Membrane Sci.,* 238 (2004) 143
6. A. A. Sapalidis, F. K. Katsaros, and N.K. Kanellopoulos, *NanoTech. Nanomater.,* 2 (2011) 30
7. C.-C. Yang, C.-T. Lin, and S.-J. Chiu, *Desalination* 233 (2008) 137
8. E. Picard, A. Vermogen, J. F. Ge´rard, and E. Espuche, *J. Membrane Sci.,* 292 (2007) 133
9. H. Zhou and J. Lee, *Acta Biomater.,* 7 (2011) 2769
10. F. Sun, H. Zhou, and J. Lee, *Acta Biomaterialia,* 7 (2011) 3813
11. J. Maiti, N. Kakati, S. H. Lee, S. H. Jee, B. Viswanathan, and Y. S. Yoon, *J. Power Sources* 216 (2012) 48
12. H. Zhang and J. Wang, *Spectrochimica Acta Part A*, 171 (2009) 1927
13. M. E. Fernandez, J. E. Castillo, F. Bedoya, J. E. Diosa, and R. A. Vargas, *Revista Mexicana de Física,* 60 (2014) 249

14. M. A. Vargas, , R.A. Vargas, and M. B. E., *Electrochim Acta,* 44 (1999) 4227
15. A. Fahmy, M. A. Abu-Saied, E. A. Kamoun, H. F. Khalil, M. E. Youssef, A. M. Attia, and F. A. Esmail, *J. Adv. Chem.,* 11 (2015) 3426
16. P. N. Gupta and K.P. Singh, *Solid State Ionics,* 86-88 (1996) 319
17. S. Mohanapriya, S. D. Bhat, A. K. Sahu, A. Manokaran, R. Vijayakumar, S. Pitchumani, P. Sridhar, and A. K. Shukla, *Energy Environ. Sci.,* 3 (2010) 1746
18. W. Xu, C. Liu, X. Xue, Y. Su,; Y. Lv, W. Xing, and T.Lu, *Solid State Ionics,* 171 (2004) 121
19. S. K. Gedam, A.P. Khandale, and S.S. Bhoga, *Ind. J. Pure Appl. Phys.,* 51 (2013) 367
20. M. Suzuki, T. Yoshida, T. Koyama, S. Kobayashi, M. Kimura, K. Hanabusa, and H. Shirai, *Polymer,* 41 (2000) 4531
21. G. H. Li, C. H. Lee, Y. M. Lee, and C. G. Cho, *Solid State Ionics,* 177 (2006) 1083
22. L. J. Lapcík, L. Lapcík, S. De-Smedt, J. Demeester, and P. Chabrecek, *Chem. Rev.,* 98 (1998)2663
23. M. B. Brown and S.A. Jones, *Europ. Acad. Dermato. Vener.,* 19 (2005)308
24. C.-C. Yang, S.J. Chiu, and C.-T. Lin, *J. Power Sources,* 177 (2008) 40
25. M. Tafaoli-Masoule, A. Bahrami, and E.M. Elsayed, *Energy*, 70 (2014) 643
26. W. Yuan, J. Deng, Z. Zhang, X. Yang, and Y. Tang, *Renew. Energy,* 62 (2014) 640
27. H. Bahrami, and A. Faghri, *J. Power Sources,* 230 (2013) 303
28. J. Ge and H. Liu, *J. Power Sources,* 160 (2006) 413
29. W. Liu and C.-Y. Wang, *J. Electrochem. Soc.,* 154 (2007) B352
30. X. Yang, Q. Liu, X. Chen, F. Yu, and Z. Zhu, *Carbohyd. Polym.,* 73 (2008) 401
31. E. Kenawy, E. A. Kamoun, M. S. Mohy Eldin, and M. A. El-Meligy, *Arab. J. Chem.,* 7 (2014) 372
32. S. Liang, L. Liu,; Q. Huang, and K. L. Yam, *Carbohyd. Polym.,* 77 (2009) 718
33. A. Fahmy, R. Mix, A. Schonhals, and J. F.Friedrich, *Plasma Process Polym.,* 8 (2011) 147
34. F. Donghtd, W. Beibei, X. Zheng, and G. Qisheng, *J. Wuhan University of Technology - Mater. Sci. Ed.,* 21 (2006) 32
35. Crank, J., *The mathematics of Diffusion.* Clarendon Press, Oxford, UK, 1975
36. T. Ebina and F. Mizukami, *Adv. Mater.,* 19 (2007) 2450
37. A. Zhu, A. Cai, J. Z. Huawei, and J. J.Wang, *J. Appl. Polym. Sci.,* 108 (2008) 2189
38. M. S. Boroglu, S. Cavus, I. Boz, and A. Ata, *Express Polym. Letters,* 5 (2011) 470